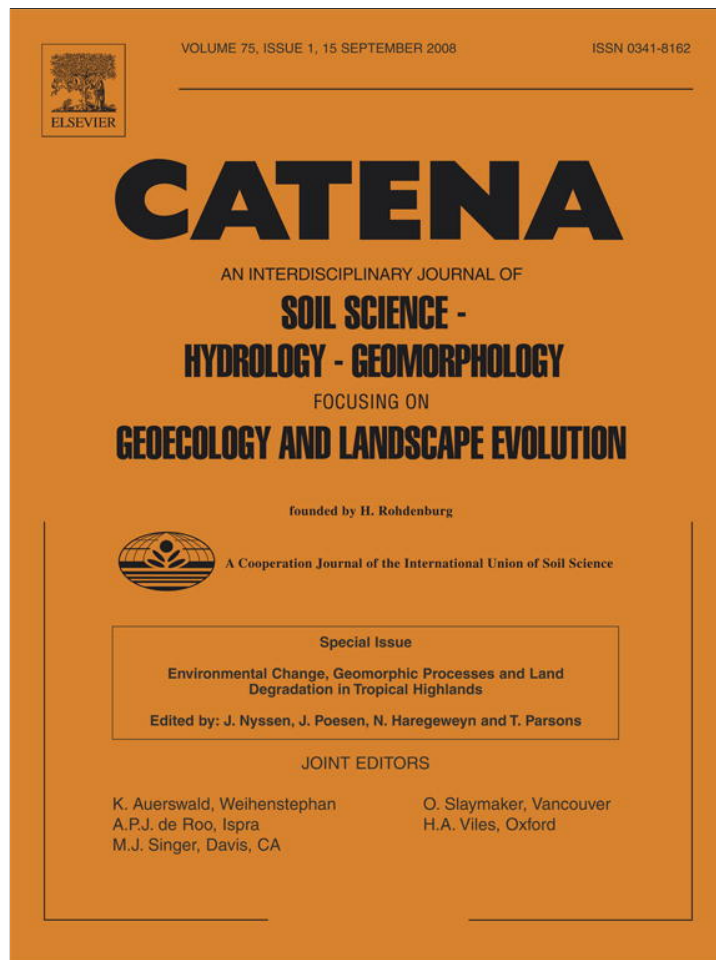


Provided for non-commercial research and education use.  
Not for reproduction, distribution or commercial use.



This article appeared in a journal published by Elsevier. The attached copy is furnished to the author for internal non-commercial research and education use, including for instruction at the authors institution and sharing with colleagues.

Other uses, including reproduction and distribution, or selling or licensing copies, or posting to personal, institutional or third party websites are prohibited.

In most cases authors are permitted to post their version of the article (e.g. in Word or Tex form) to their personal website or institutional repository. Authors requiring further information regarding Elsevier's archiving and manuscript policies are encouraged to visit:

<http://www.elsevier.com/copyright>



Contents lists available at ScienceDirect

Catena

journal homepage: [www.elsevier.com/locate/catena](http://www.elsevier.com/locate/catena)

## Stratigraphy of near-valley head quaternary deposits and evidence of climate-driven slope-channel processes in southern Brazilian highlands

Marcelo Accioly Teixeira de Oliveira <sup>a,\*</sup>, Hermann Behling <sup>b</sup>, Luiz Carlos Ruiz Pessenda <sup>c</sup>, Gisele Leite de Lima <sup>a</sup>

<sup>a</sup> Departamento de Geociências, CFH, Universidade Federal de Santa Catarina (UFSC), Caixa Postal 5175, cep: 88040-970, Trindade, Florianópolis, Santa Catarina, Brazil

<sup>b</sup> Department of Palynology and Climate Dynamics, Albrecht-von-Haller-Institute for Plant Sciences, University of Göttingen, Untere Karspüle 2, D-37073, Göttingen, Germany

<sup>c</sup> Centro de Energia Nuclear na Agricultura, Laboratório de C 14, Universidade de São Paulo (USP), Avenida Centenário no. 303, São Dimas, cep: 13416000, Piracicaba, São Paulo, Brazil

### ARTICLE INFO

#### Keywords:

Colluvium  
Stratigraphy  
Quaternary  
Climate changes  
Environmental changes

### ABSTRACT

During the past 40 years colluvial and alluvial deposits have been used in Brazil as good indicators of regional landscape sensitivity to Quaternary environmental changes. In spite of the low resolution of most of the continental sedimentary record, geomorphology and sedimentology may favor palaeoenvironmental interpretation when supported by independent proxy data. This paper presents results obtained from pedostratigraphic sequences, in near-valley head sites of southern Brazilian highlands, based on geomorphologic, sedimentologic, micromorphologic, isotopic and palynologic data. Results point to environmental changes, with ages that coincide with Marine Isotopic Stages (MIS) 5b; 3; 2 and 1. During the late Pleistocene, although under temperatures and precipitation lower than today, the local record points to relatively wet local environments, where shallow soil-water saturated zones contributed to erosion and sedimentation during periods of climatic change, as during the transition between MIS 2 and MIS 1. Late Pleistocene events with ages that coincide with the Northern Hemisphere Younger Dryas are also depicted. During the mid Holocene, slope-wash deposits suggest a climate drier than today, probably under the influence of seasonally contrasted precipitation regimes. The predominance of overland flow-related sedimentary deposits suggests an excess of precipitation over evaporation that influenced local palaeohydrology. This environmental condition seems to be recurrent and explains how slope morphology had influenced pedogenesis and sedimentation in the study area. Due to relative sensitiveness, resilience and short source-to-sink sedimentary pathways, near-valley head sites deserve further attention in Quaternary studies in the humid tropics.

© 2008 Elsevier B.V. All rights reserved.

### 1. Introduction

During the past 40 years the study of erosive and sedimentary processes in topographic hollows has been a common topic for Brazilian research in geomorphology and quaternary geology (Bigarella and Mousinho, 1965; Meis and Machado, 1978; Meis and Moura, 1984; Moura et al., 1991). Since the 1960s, the role of the so-called colluvial ramps as slope-channel coupling landforms is emphasized on the basis of sedimentary evidence (Bigarella and Mousinho, 1965; Meis and Moura, 1984). More recently, the role of topographic hollows connected to the drainage network was approached into the far-reaching theoretical framework of the channel-heads characterization and modeling (Dietrich and Dunne, 1993). Erosive and sedimentary cycles and hemicycles, surges of geomorphic processes and their connection to environmental controlling factors are important issues for geomorphology and Quaternary geology studies because they allow drawing inferences about climatic teleconnections and millennial oscillations that seem realistic in terms of the information

produced by proxy ice-core records (Aharon and Chappell, 1986; Coltrinari, 1993; Iriondo, 1999; Thomas, 2004).

As proposed earlier (Bigarella and Mousinho, 1965; Meis and Monteiro, 1979), alluvial and colluvial deposits are widely recognized today as good indicators of local and regional landscape sensitivity to environmental changes in the humid tropics (Thomas, 2004). They allow the establishment of formal quaternary stratigraphic units (Moura and Mello, 1991; Melo et al., 2001) and a characterization of the responses of landforms to regional expressions of global changes (Servant et al., 1989; Moura et al., 1991; Turcq et al., 1997; Stevaux and Santos, 1998; Modenesi-Gauttieri, 2000).

However, although colluvial deposits are widely spread features in tropical and subtropical Brazil (Melo and Cuchierato, 2004), direct correlative proxy data is usually scarce (e.g. Turcq et al., 1997), making difficult the definition of relationships between landform evolution, controlling environmental factors and global climatic changes. In addition, due to the main processes at work on slopes, the general scarcity and low resolution of the quaternary continental record (Thomas and Thorp, 1996; Thomas et al., 2001) tend to be enhanced in colluvial mantles, since ephemeral flows usually produce unorganized sediments, preventing sound interpretation (Bertran and Texier, 1999;

\* Corresponding author. Tel.: +55 48 37218583; fax: +55 48 37219983.  
E-mail address: [maroliv@cfh.ufsc.br](mailto:maroliv@cfh.ufsc.br) (M.A.T. de Oliveira).

Nemec and Kazanci, 1999, Bertran and Jomelli, 2000; Fard, 2001). In this context, the identification of particularly sensitive terrains and landforms in which climate-driven erosive and sedimentary events may be produced and preserved seems to be crucial (Thomas, 2004).

Due to its territorial dimensions, Brazilian lands are under the influence of several climatic regimes, ranging from equatorial and tropical, to mild subtropical climates. This article presents a study of colluvial and alluvial mantles in southern Brazilian subtropical highlands, where mild climates now predominate. Geomorphologic, stratigraphic, sedimentologic, geochronologic, palynologic, isotopic and micromorphologic data, obtained from three near-valley head sedimentary sequences are presented. Since the study sites are located near valley head areas, the fact that these geomorphic units are effective sources of information for Quaternary interpretation is enhanced (Moura et al., 1991; Dietrich and Dunne, 1993).

## 2. Setting, material and methods

The study sites are located in the northern highlands of Santa Catarina State, in southern Brazil, in the municipality of Campo Alegre (Fig. 1). Campo Alegre is located in the “São Bento do Sul” Plateau, which is characterized by a rocky, stepped, hilly landscape, strongly influenced by differential weathering and erosion, displaying cuesta-like fronts along the Plateau’s border. Neoproterozoic trachytes, rhyolites and ignimbrites from the Campo Alegre volcano-sedimentary basin compose the local bedrocks (Biondi et al., 2001). Weathering of these rocks gives place to important clay deposits, probably influencing morphogenesis during the Quaternary, as deep alteration mantles are common, together with colluvium and alluvium and soils.

Local altitudes range from 850 to 1200 m a.s.l. and the climate is mesothermic, with relatively temperate summers (Köppen’s Cfb type). The mean annual temperature is about 16.4 °C and mean precipitation varies from 1600 to 1800 mm per year. Tropical and subtropical vegetation coexist in the region, forming the so-called *Araucaria* forest (Mixed Ombrophic Forest). Natural and introduced grasslands are also frequent, with gallery forests extending along hollows and valleys (Oliveira and Pereira, 1998). Preliminary geomorphologic surveys in the area had revealed important quaternary deposits preserved in hollows and valley heads (Oliveira et al., 2001). Colluvium, alluvium and buried peat deposits and soil epipedons bear evidence of local environmental changes, the timing of which embraces, so far, a relatively large span of the Last Glacial Cycle (LGC).

Pedostratigraphic sequences were identified and described in the field (Finkl, 1984). Colluvial and alluvial deposits, interstratified with

buried epipedons and peat horizons, constitute the main features observed. Since the terms “colluvium” and “alluvium” may vary in the literature, they are used here in their broad senses to mean, respectively, detritus transported by various processes on slopes and detrital material transported by streams or rivers. The expression “valley head” is used as an equivalent to “hollow” and “unchanneled valley” to mean topographic convergent areas, upslope of the channel network, in which channelized and unchannelized sediment transport may occur. When slope and stream sediments happen to be mixed in the same site as, for instance, near a valley head environment (Dietrich and Dunne, 1993), they are referred to as colluvial–alluvial deposits.

Sedimentary units and buried epipedons were described according to their color, thickness, geometry, texture and gravel content. Samples were systematically taken from both sediments and soils for several studies. Textural analyses were conducted according to standard procedures (Lima, 2005) and the results were displayed on ternary plots for classification. Muddy samples were classified following Flemming (2000) and samples with important gravel content (more than 5%) were classified according to Folk (1974). In some instances, textural data is displayed as the textural index ( $\%_{<2\ \mu\text{m}} \cdot \%_{>10\ \mu\text{m}}$ ), which expresses a ratio between the relative proportion of grains smaller than 2  $\mu\text{m}$  and those larger than 10  $\mu\text{m}$ . Samples which are mainly composed of weathered lithic fragments, or alterorelicts, were impregnated with polyester resin for analysis under polarizing microscopy (Scholle, 1979; Bullock et al., 1985; Delvigne, 1998). When judged appropriate, analysis between macroscopic and microscopic scales of thin lenses was made with the use of digital images (De Keyser, 1999) obtained from a CanoScan-2710 slide-scanner device.

Soil carbon analysis of buried soil samples (total organic C and  $^{13}\text{C}$ ) was carried out at the Stable Isotope Laboratory of the Centre for Nuclear Energy in Agriculture (CENA), in Piracicaba, Brazil. The organic carbon results are expressed as a percentage of dry weight.  $^{13}\text{C}$  results are expressed as  $\delta^{13}\text{C}$  with respect to PDB standard using the conventional  $\delta$  (‰) notations:

$$\delta^{13}\text{C}(\text{‰}) = [(R_{\text{sample}}/R_{\text{standard}}) - 1] \cdot 1000 \quad (1)$$

where  $R_{\text{sample}}$  and  $R_{\text{standard}}$  are the  $^{13}\text{C}/^{12}\text{C}$  ratio of the sample and standard, respectively. Analytical precision is  $\pm 0.2\text{‰}$  (Pessenda et al., 2004).

Excavated organic deposits were sampled for pollen analysis in two sedimentary sequences. Twenty-four (24) samples of 0.5  $\text{cm}^3$ , at 10 cm intervals along 150 cm and 75 cm core samples were collected in plastic bags and stored under cool (ca. +8 °C) and dark conditions

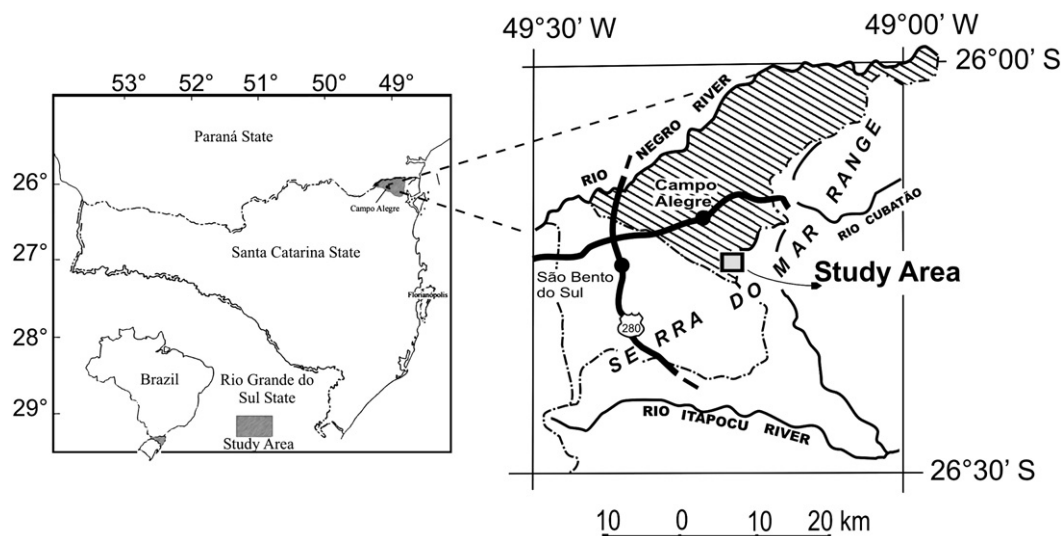


Fig. 1. Study area location.

after their return from the field. Samples were processed with standard pollen analysis methods, using HF (78%) and acetolysis. To determine the pollen concentration, one tablet of exotic *Lycopodium clavatum* spores was added to each sample. A minimum of 300 pollen grains were counted. For pollen identification, the Behling's pollen collection was used (containing about 2000 Brazilian species) together with pollen morphological descriptions (Behling, 1993). For plotting of the pollen data, calculations and cluster analysis TILIA, TILIAGRAPH and CONISS software was used (Grimm, 1987).

Radiocarbon ages were determined at Beta Analytic Incorporation (USA); at the Institute of Physics of the Erlangen-Nürnberg University (Germany) and at <sup>14</sup>C Laboratory of CENA, University of São Paulo – Piracicaba (Brazil). Thermoluminescence (TL) and optic stimulated luminescence (OSL) ages were obtained at the Laboratory of Glasses and Dating from the Faculty of Technology of São Paulo (FATECSP – Brazil).

### 3. Results and analysis

#### 3.1. The stratigraphic record

Three pedostratigraphic sequences are reported. Distances between each sequence vary from about 0.5 to 1.5 km, embracing an area of approximately 4 km<sup>2</sup>. All reported sequences are located between the Rio Itapocu river basin and the Rio Negro river basin, in small first order catchments (see Fig. 1). The Itapocu River flows to the east, along the local “Serra do Mar” range escarpment, and the Negro River is a tributary of the Iguaçu River which flows to the west, from the western flank of the “Serra do Mar” range, entering the Paraná River and reaching the Atlantic Ocean along the coast of Uruguay and Argentina, in the “La Plata” estuary. Results are presented according to the relative increase in distance of each sedimentary sequence from the drainage divides.

##### 3.1.1. Near-divide sedimentary sequence

The pedostratigraphic sequence illustrated in Fig. 2 was preserved near the drainage divides of the so-called “Cerro do Touro” hill, one of the highest summits in the study area. The sequence is part of a system of colluvial ramps, which remain perched over a dissected first order valley.

Colluvial lenses and layers intercalate with thick buried epipedons (pedostratigraphic units 5 and 11 of Fig. 2). The sequence is truncated at the centre of the figure by channel-like features, constituting cut-and-fill sedimentary structures, filled by undifferentiated colluvium,

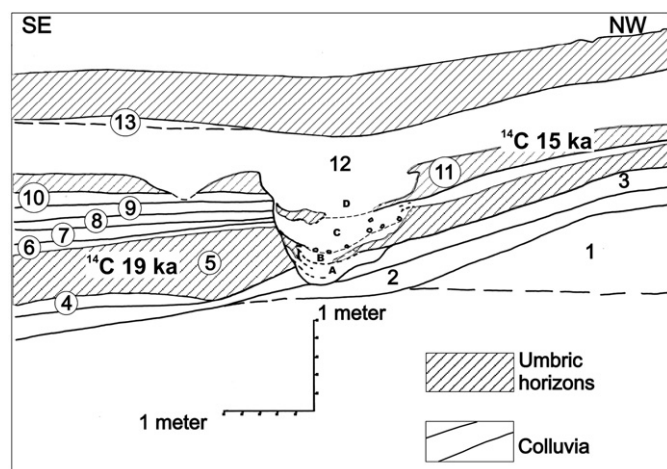


Fig. 2. Schematic illustration of the pedostratigraphic sequence, which is located near the divides. Numbers correspond to main sedimentary units. Note the apparent increase in the volume of sediments, which is suggested by the increasing width of the gully infilling sets (A, B, C, D) upwards.

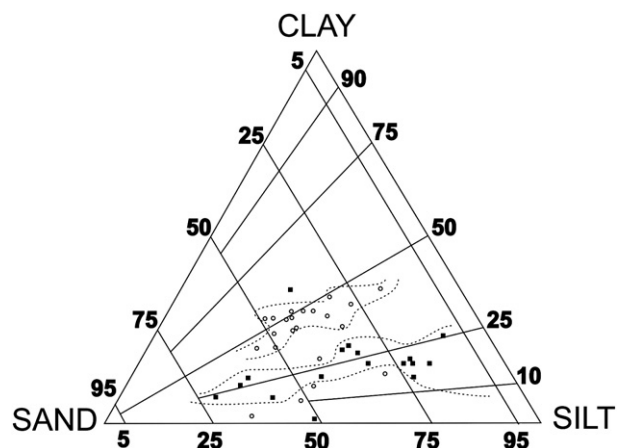


Fig. 3. Distribution of samples in the Flemming diagram. Squares indicate samples from buried epipedons. Circles indicate colluvial samples. Different genetic materials tend to cluster in different zones of the diagram.

the geometry of which follows the present topography. The sequence ends up with the present-day thick umbric epipedon at the top. Textural classification of materials from this section may be observed in Fig. 3.

As expected, different materials tend to distribute along different zones of the diagram, contributing to faciologic analysis (Flemming, 2000; Oliveira and Lima, 2004). Material from colluvial units are grouped around the centre of the diagram, while samples under the influence of pedogenesis are distributed along a wider range of textural classes, depending on their silt content. Gravel content in colluvial samples ranges from 4.3% to 12.38%, falling to 0.41% in samples from the buried palaeosoils.

According to radiocarbon ages (Table 1), unit 5 was probably developed during the Last Glacial Maximum (LGM) and unit 11 during a period between the LGM and the Holocene. No vegetal remnants were identified inside these buried epipedons and pollen analysis showed only degraded pollen grains, precluding pollinic study. The black color of the horizons (10YR 2/1) and their carbon content indicates buried umbric epipedons (Lima, 2005). Soil carbon content and  $\delta^{13}\text{C}$  soil carbon content of the set buried soils are displayed below (Fig. 4).  $\delta^{13}\text{C}$  values indicate a mixture of C<sub>3</sub> type (trees) and C<sub>4</sub> type (grass) vegetation in both palaeosol horizons. These soil organic matter (SOM) results indicate the presence of herbs and trees, which is typical of the Brazilian Cerrado/Campos transition.

According to the topographic position of the sequence, SOM analysis suggests that trees and bushes were established near the water divides of the study site, during the LGM. In addition, stratigraphy and radiocarbon dates suggest a change of sedimentary pattern along the sequence. Before and around the LGM, probably under the influence of diffusive mass movements and low temperatures, colluvial lenses and layers intercalated to thick umbric epipedons (see Fig. 2). After the LGM, evidence suggests that gully erosion produced cut-and-fill structures that were quickly buried under a thick colluvial layer. This gully erosion episode took place after <sup>14</sup>C 15,260 ± 80 years BP, probably documenting a change of the site's

Table 1  
Data for radiocarbon ages of the watershed sequence samples

Laboratory code (#)	Beta-124761	Beta-106474
Field code (#)	CA.24-10.A1	CA.S-1
Depth of the sample (m)	1.2	2.2
Stratigraphic unit	11	5
Analysis	AMS	AMS
Age ( <sup>14</sup> C years BP)	15,260 ± 80	19,130 ± 110
$\delta^{13}\text{C}$ (‰)	-25.0	-25.0

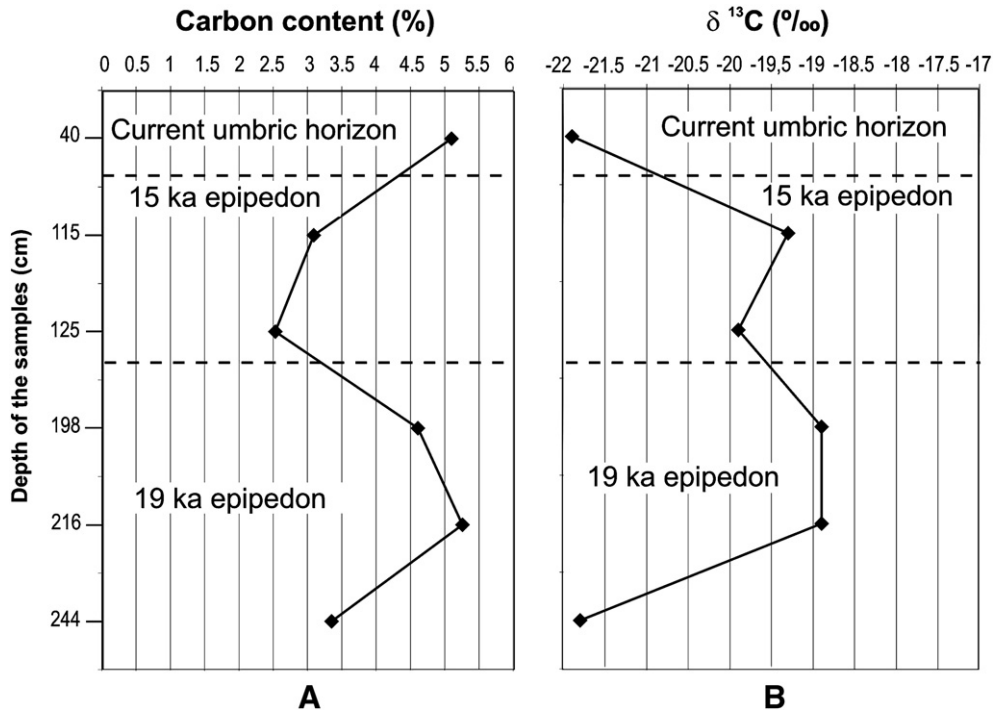


Fig. 4. Soil organic carbon content and  $\delta^{13}\text{C}$  values of the watershed site buried soils. Generally,  $\delta^{13}\text{C}$  values range from  $-30$  to  $-22$  per thousand for  $\text{C}_3$  type plants (trees) and from  $-17$  to  $-9$  for  $\text{C}_4$  type ones (grass).

hydrologic pattern, passing from diffusive mass movements to concentrated overland flows. The evident increase in thickness of the last colluvial layer (unit 12), combined with increasing amounts of infilling material in the main gully incision (A, B, C, D subunits), suggest a period of increasing local sedimentation on the slope.

### 3.1.2. Valley head sedimentary sequence

The sequence illustrated in Fig. 5 was surveyed at the inner downslope border of a clay quarry. It represents a typical accretionary valley head environment, in which episodic erosion and sedimentation had intercalated with soil development and slow decomposition of organic matter, under the influence of shallow water-table levels. Further details on  $^{14}\text{C}$ , OSL and TL ages are given in Tables 2 and 3, respectively.

The set begins, at the base, with a 30 to 50 cm thick colluvial layer composed of sub-parallel lenses of weathered gravels, displaying subsidiary cross-lamination (unit 1). This unit rests dis-

cordantly over the deeply weathered neoproterozoic pyroclastic bedrock and probably dates from an early LGC period (TL  $90,000 \pm 11,000$  years BP). An abrupt but continual muddy transition above led to a buried peat bog, 150 cm thick (unit 2). The ages obtained for unit 2 suggests that the upper part of the unit was probably formed during marine isotope stage number 3 (MIS 3), while the lower part is apparently older than the limit of radiocarbon dating (Tables 2 and 3).

Unit 2 peat bog is covered by about 1.5 m of undifferentiated mud material, strongly altered by hydromorphy (unit 3). The top of this hydromorphic unit preserves remnants of a buried ochric epipedon truncated by erosion (unit 4) (Fig. 5). A lag deposit composed of well-sorted coarse sands is found along the resulting stratigraphic disconformity. This sandy deposit was dated by OSL as  $6625 \pm 750$  years old and marks the limit between pleistocenic and holocenic sequences at this site. The lag deposit is covered by 75 cm of muddy gravel material, displaying normal grading (unit 5). The

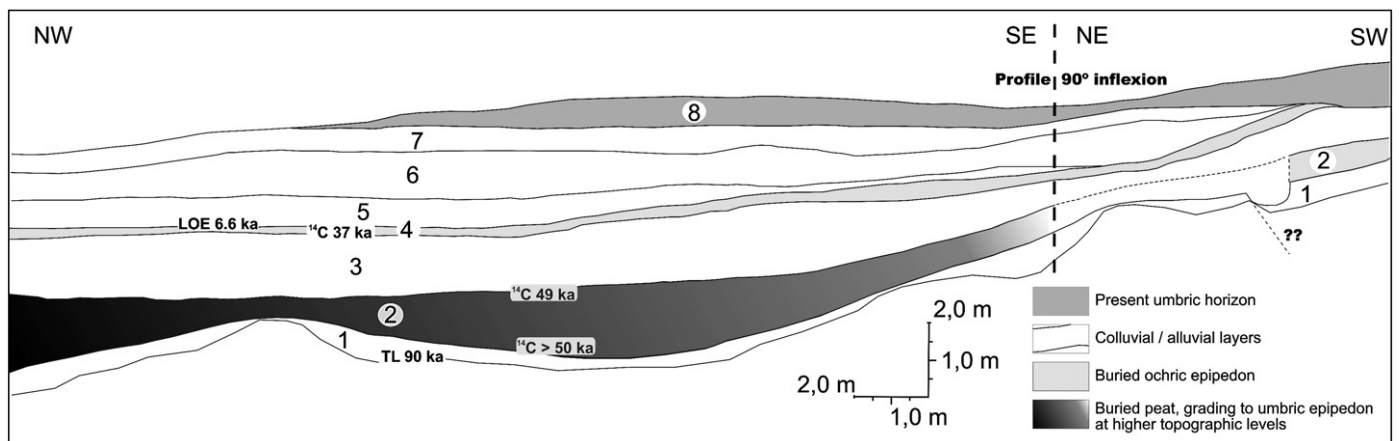


Fig. 5. Schematic representation of the valley head pedostratigraphic sequence. The numbers correspond to main sedimentary units. Note the general concave geometry of the lower sedimentary units and the general convexity of the upper ones.

**Table 2**  
Data for radiocarbon ages of the valley head sequence samples

Laboratory code (#)	# 953/CENA # 520	# 851/CENA # 444	Erl-5456
Field code (#)	Paleo-2	CA-TOPO	PH-09/02-2
Depth of the sample (m)	2.5	5.4	6.9
Stratigraphic unit	4	2 (top)	2 (base)
Analysis	AMS	Radiometric	AMS
Age ( $^{14}\text{C}$ years BP)	37,000 ± 1425	49,300 + 9700 – 4250	> 50,000
$\delta^{13}\text{C}$ (‰)	–19.5	–29.0	–28.82

sedimentary set terminates with 2.5 m of very-finely-stratified colluvium, made up of alternated lenses of weathered gravel, sand and silt sized particles (units 6 and 7). The dates obtained allow dividing the sequence into two different sub-sequences, the first from the Pleistocene (units 1, 2, 3 and 4) and the second from the Holocene (units 5, 6, 7 and 8).

**3.1.2.1. Results from the pleistocenic units.** Detailed textural analysis was performed on samples of units 2, 3, 4 and 6. The buried peat deposit (unit 2) was subjected to detailed sedimentologic and palynologic investigation. Textural classification of unit 2 materials is illustrated in Fig. 6. Viewed as a whole, samples of unit 2 may be grouped in two separate levels: an inferior, texturally coarser level and a superior, texturally finer level, as illustrated in Fig. 7. The two textural levels are separated at a depth of approximately 590 cm by a strong enrichment in clay-sized material.

The summary pollen percentage diagram of a core taken from this peat layer (unit 2), including pollen concentration and the cluster analysis dendrogram, shows that the pollen diagram also can be divided into two local pollen zones: respectively, zone I and zone II (Fig. 8). The pollen percentage diagram shows the major significant taxa based on the total pollen sum (Fig. 9). Identified pollen taxa were grouped into Campos, *Araucaria* forest and Atlantic rain forest.

Pollen zone I (150–45 cm, 11 samples) is characterized by abundant Campos (grassland) pollen taxa (60–67%), primarily Poaceae, followed by Cyperaceae, *Baccharis*, and Asteraceae subf. Asterioideae and other taxa such as Apiaceae, *Eryngium* and *Valeriana*, which occur in lower percentages. *Araucaria* Forest pollen sums are moderate (25–32%), represented primarily by Myrtaceae, followed by *Podocarpus*, *Weinmannia*, Melastomataceae, *Myrsine*, *Ilex*, *Symplocos* and *Daphnopsis*. Pollen grains of *Araucaria angustifolia*, except one single grain, are missing. Percentages of Atlantic Rain Forest pollen taxa are low (1–3%) and represented only by single grains such as *Alchornea*, *Celtis* and Moraceae/Urticaceae. Aquatic pollen taxa are absent or were found only in single grains. Tree fern spores of *Cyathea* and *Dicksonia* are recorded in low percentages. Other fern spores are more frequent, primarily represented by the *Blechnum imperiale*-type and monlete psilate spores. Percentages of moss spore are rare.

In pollen zone II (45–0 cm, 5 samples) pollen grains represent the Campos vegetation, which are continuously predominant along the sequence (60–70%). Percentages of *Eryngium* and some other Campos pollen taxa are somewhat lower, while other taxa remain unchanged. The sum of the *Araucaria* Forest group is similar to zone I, but the

**Table 3**  
Data for luminescence ages of the valley head sequence samples

Laboratory code (#)	LVD-1127	LVD-662
Field code (#)	CA-base-LOE	CA-SC-73
Depth of the sample (m)	3.4	7.5
Stratigraphic unit	Lag deposit	1 (base)
Dating method	OSL	TL
Annual dose ( $\mu\text{Gy/yr}$ )	436 ± 40	1800 ± 40
P (Gy)	2.89	150
Age (years)	6625 ± 750	90,000 ± 11,000

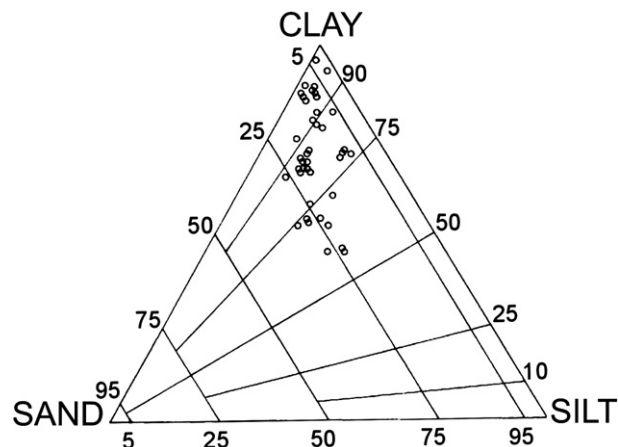


**Fig. 6.** Flemming textural classification of materials from unit 2 buried peat bog. Most of the peat material is characterized as Flemming type sandy mud (50 to 75% of mud), slightly sandy mud (75–95% of mud) and mud (>95% of mud).

composition changed, as Myrtaceae percentage is slightly lower than in zone I, and percentages of *Podocarpus* are markedly higher. Also, percentages of *Weinmannia* became rare. Percentages of the group of Atlantic Forest taxa remain at low levels (1–2%), but pollen of Melastomataceae/Combretaceae decreases, while *Myrsine* increases. Tree fern spores and the *Blechnum imperiale*-type decrease in this zone.

This pollen record suggests a change in composition along unit 2 from an older period of relatively drier and warmer climate (pollen zone I), to a younger period of wetter and colder climate (pollen zone II). This inference is based on the higher percentages of *Podocarpus* and the rare occurrence of *Weinmannia* in the younger pollen zone II. Indeed, *Podocarpus* needs relatively wet environment for growth and *Weinmannia* would be sensitive to lower LGC temperatures (Behling, 1993).

The  $\delta^{13}\text{C}$  analysis of unit 2 suggests the predominance of tree species, or  $\text{C}_3$  type grasses as Cyperaceae, along the entire unit (Fig. 10). Total carbon content decreases continuously from the base to the top of the profile. The association of  $\text{C}_3$  grasses and trees in unit 2, the age of which coincides at least with MIS 3, may be explained either as a consequence of early MIS 3 general interstadial trend, or as a consequence of the local concave topography of the buried valley head, making a transitive environment between grasslands in the summits and gallery forests in the valleys.

Units 3 and 4 are mainly constituted by material classified as clayey slightly sandy mud, suggesting an apparent low energy environment for deposition of unit 3. Unit 4 radiocarbon age indicates that this soil epipedon had developed by the end of MIS 3 (Table 2). SOM data obtained from this unit is also displayed in Fig. 10, where more enriched  $\delta^{13}\text{C}$  values indicate the presence of less dense vegetation, probably with  $\text{C}_4$  type herbs increasing in importance. Globally, SOM results coincide with pollen data (Figs. 8 and 9), suggesting the predominance of a relatively wet local climate condition during the formation of the LGC peat bog (unit 2), which was followed by a relatively local climatic degradation, probably due to increasing dryness, leading to the formation of unit 3 altered muddy material and to unit 4 ochric epipedon, usually formed under warmer conditions in Brazil.

These results suggest that periods of erosion and sedimentation had alternated with periods of soil development, in a local environment where a shallow water table gave rise to peat accumulation, slow deposition and hydromorphic weathering. This local soil saturated pedoclimatic condition had probably prevailed during the early MIS 3 interstadial, by the end of which deposits and soils of unit 3 and 4, together with SOM data, bear evidence of increasing dryness.

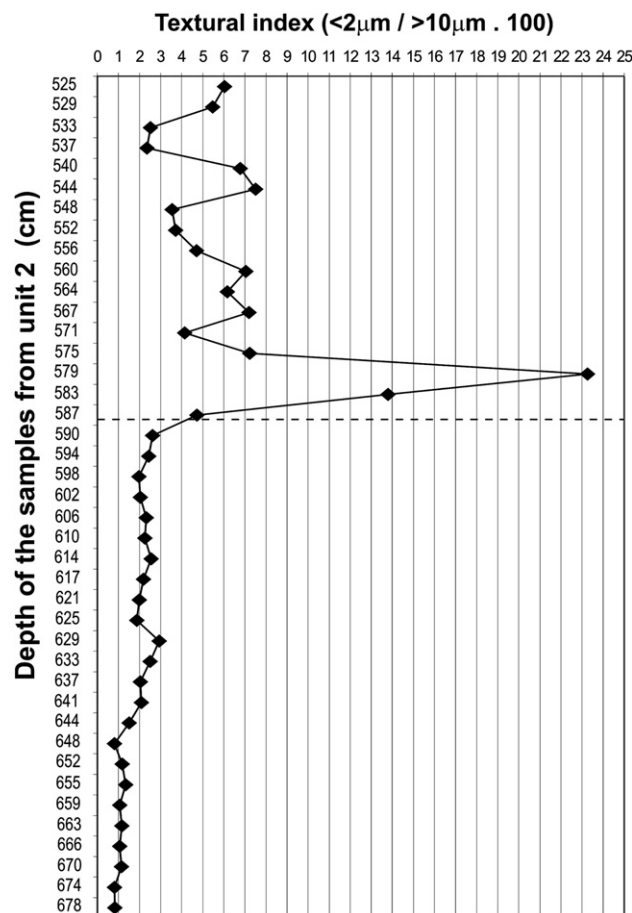


Fig. 7. Grain size ratio ( $<2\mu\text{m} / >10\mu\text{m}$ ) estimated at 5 cm intervals for the 150 cm long peat bog.

**3.1.2.2. Results from the holocenic units.** The beginning of the set holocenic sequence is marked by the erosive discontinuity over the unit 4 ochric epipedon. LOE dating of the lag deposit along the discontinuity suggests that unit 4 was truncated by erosion during the Mid Holocene (see Table 3). The first deposit over the erosive discontinuity is a 75 cm thick normal graded layer of muddy gravel (unit 5). This layer is covered by about 2.5 m of finely stratified colluvial/alluvial material composed of alternated lenses of gravel, sand and mud (units 6 and 7) (see Fig. 5). Since clasts of these layers are completely weathered, forming loose alterorelicts (*sensu* Delvigne, 1998), their textural analysis was conducted by optic microscopy. Samples from the erosive discontinuity and from units 5 and 6 were analyzed.

Results of the micromorphologic analysis of samples from this transition and from samples of unit 5 and 6 suggest: a) shearing near the top of the buried truncated epipedon (unit 4); b) relatively rapid local burying, following erosion of unit 4; c) carbonized small roots in pedotubules of unit 4; d) clastic deposition inside unit 4 cracks and e) post-depositional weathering of overlaying units (units 5 and 6) (Oliveira et al., 2006).

Unit 6 is composed of alternated lenses of mud and gravel. If plotted in ternary diagrams for textural classification, the muddy subunits would be classified as Flemming's clayey sandy mud (C–V) and very clayey slightly sandy mud (D–V), while the gravelly subunits would classify as gravelly mud, muddy gravel and gravelly muddy sand, according to Folk's ternary diagram (Folk, 1974). Fig. 11 illustrates scanned images of thin lenses obtained from a sample of unit 6 (Fig. 11A) and from one sample of contemporary rain-wash deposits (Fig. 11B). The latter was created over the bare floor of the study site clay quarry (Fig. 12), about 50 m from the pedostratigraphic sequence, after three days of rain, amounting to about 59.7 mm. Clastic material

from holocenic and contemporary deposits of Fig. 11 seem to come from the same source area.

A comparison of the scanned thin lenses shows similar structures, although some important differences may be noted (Table 4). Alternation of coarse and fine lamina is common in both holocenic and contemporary samples. Inner detailed structures show that the holocenic sample (Fig. 11A) is mainly composed of discrete massive and compacted lamina of mud, sands and gravel, since 67% of the laminae are massive (units 1, 2, 3, 4, 6, 9', 10, 11), while 33% display preferential organization (units 5, 7, 8, 9) (Table 4). The present-day rain-wash sample (Fig. 11B) has 53% of massive lamina (units 1, 2, 3, 4, 7, 8, 13), while 47% are better organized (units 5, 6, 10, 10', 11, 12, 14) (Table 4). Massive and preferentially organized lamina in the contemporary sample present a more openly-packed framework structure, mainly composed of sand, gravel and some mud.

The geometry of lamina in both samples shows that fine gravel and coarse sand compose lenticular bodies, while fine sand and mud tend to make parallel-sided lamina (Fig. 11), eventually developing inner lamination, clearly visible under microscopy. The holocenic deposit displays better sorting and better inner organization in finer sediments (fine sands and mud), while poor sorting and massive lenses are mainly made by coarser sediments (Table 4). The contemporary deposit does not display any clear textural relationship, in spite of a tendency to improve inner organization in the lower mode matrix-supported lamina (Table 4).

The two samples have a similar geometry of coarse and fine lamina and lenses. In general, the inner organization is quite similar, although a slight majority of massive lamina is observed in the holocenic sample. In spite of this, the holocenic lamina have a strong correlation between grain size and sorting ( $r=0.72$ ), while the

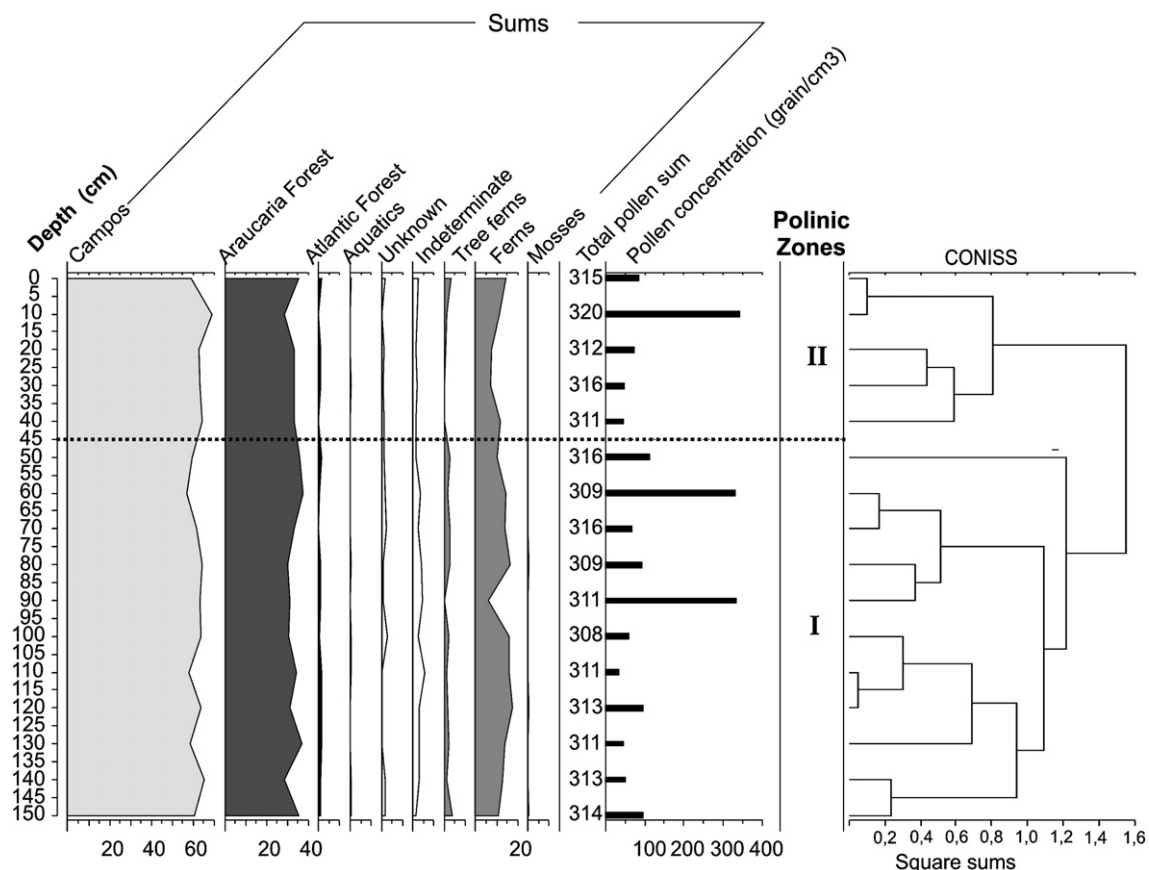


Fig. 8. Summary pollen percentage diagram, including pollen concentration and the cluster analysis dendrogram, of the buried peat bog.

contemporary lamina display no significant correlation between textural characteristics (Table 4). In addition, the holocenic lamina are slightly better sorted than the contemporary ones (67% of holocenic and 60% of contemporary lamina classify as well to very well sorted sediments).

Little doubt exists about the origin of the contemporary deposit, since it is the fresh result of rain-washing flows, witnessed in the field (Fig. 12). Concerning the holocenic deposit, if we take into account, first, its depositional setting (an unchanneled swale); second, the general structural similarities between coarse and fine lamina in holocenic and contemporary samples; third, the general description of the holocenic deposits at the stratigraphic section, we must suggest: a) that both contemporary and holocenic deposits are typically slope wash deposits; b) that rain-washing flow is the main depositional agent in both cases (Oliveira et al., 2006). This suggestion is also supported by the differences between the two samples: a) the pluvial contemporary deposit is better organized, although poorly sorted, probably due to the continuous variation of precipitation rates during the three rainy days recorded, leading to mechanical sieving and impregnation of coarser sediments by finer ones, during lowering flow rates (Ferreira and Oliveira, 2006); b) the torrential holocenic deposit is mainly massive, although better sorted, suggesting sporadic variable pulses of precipitation with rapid deposition, which are characteristic of drier environments. Indeed, massive, parallel laminated and graded sandy laminae are all indicative of depositional processes associated with fluctuations of fluid flow strength. Massive and laminated sands, which predominate in the holocenic sample, indicate rapid deposition, while grading, more frequent in the contemporary sample, is usually associated with fluctuations in flow energy. Considering this evidence, general and detailed structures found in the holocenic Unit 6, of this valley head sequence, suggest that the holocenic units were formed in an alluvial

fan-like setting, during the early to mid Holocene, under the influence of rain-washing flow.

As a result, the holocenic sequence reveals deposits that had probably formed under the influence of pulses of rain-washing over the adjacent slopes of the study valley head, implying local footslope aggradation in a sedimentary setting that was probably marked by long dry seasons during the mid Holocene. Indeed, relative dryness is required to explain such deposits, since it causes the necessary rarefaction of vegetation for rain-washing flows over relatively bare slope surfaces, building up alluvial fan structures (see Fig. 12).

### 3.1.3. Valley bottom sedimentary sequence

The sedimentary sequence is located about 700 m downslope from the near-divide study site (see Section 3.1.1 above), and pertains to the same drainage system. The sequence was built up in an alluvial fill, at a reach where the deep incised first order valley widens, upslope from a local rocky base level. As suggested by Fig. 13, the sedimentary sequence looks like a typical floodplain deposit with alternating channel fill sands and overbank mud (Miall, 1985).

The sequence begins with a colluvial layer, set over one of the side-slopes of the valley floor (unit 1). An undated umbric epipedon evolved over this layer (unit 2) (Lima, 2005), before it was buried under a second colluvial layer (unit 3). Erosion of colluvia, soil and valley floor probably preceded deposition of the sandy and gravel onlapping alluvial lenses of units 4 and 5. The unit 5 gravel layer preserves plant material inside, resting discordantly over the previous units. A peat deposit was developed over these gravels (unit 6), which was partially truncated by erosion, probably in association with the deposition of a channel fill (unit 7), marking the beginning of the floodplain deposits. A series of overbank clayey and silty deposits follows (units 8, 10, 12, 13, 15, 16 and 17), alternated with sandy lenses (units 9, 11 and 14). Unit 18 is the current epipedon, which is already



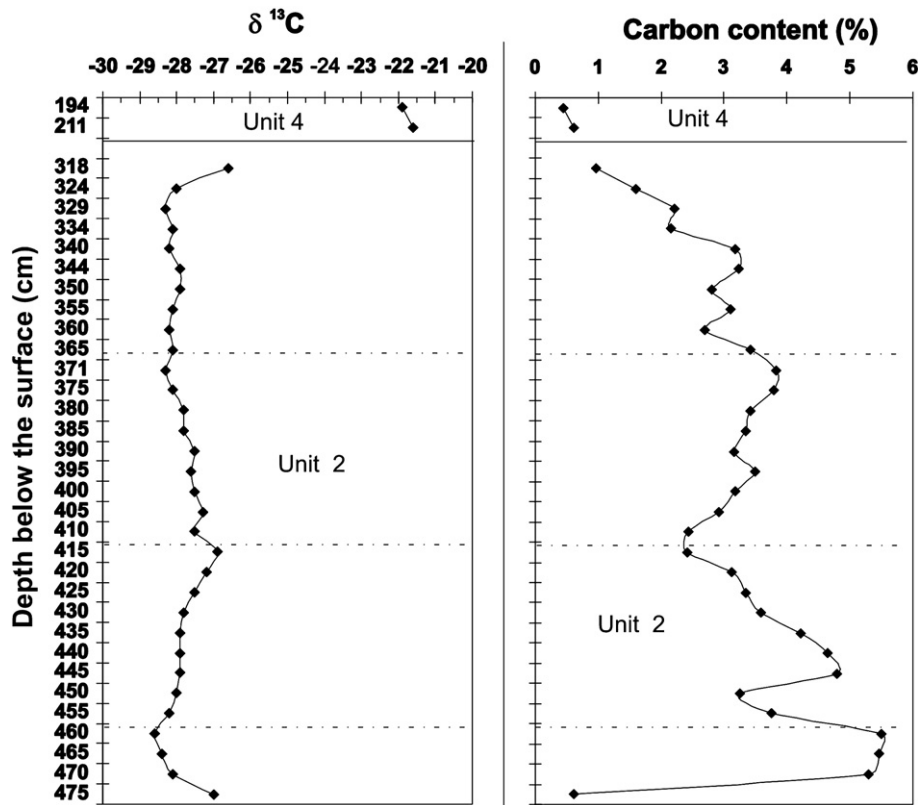


**Fig. 10.**  $\delta^{13}\text{C}$  soil carbon values and organic carbon content of unit 2 site buried peat in the valley head sedimentary sequence. Generally,  $\delta^{13}\text{C}$  values range from  $-30$  to  $-22$  per thousand for  $\text{C}_3$  type plants (trees) and from  $-17$  to  $-9$  for  $\text{C}_4$  type ones (grass).

partially buried under a thin and discontinuous layer of colluvium from the adjacent side-slope (unit 19). Further details on  $^{14}\text{C}$  and TL ages obtained from materials of the sequence are given in Tables 5 and 6 respectively.

The textural classification of materials in the sequence is illustrated in Fig. 14. Most of the deposit is composed of muddy material. Overbank sediments and buried epipedons range from Flemming textural types, slightly sandy mud (D) to mud (E), while

channel fill sediments range from sandy mud (C) to muddy sand (B), plotting in different domains of the diagram. The gravel content of sediments varies from 10% to 50% in colluvial samples and does not exceed 5% in alluvial samples. There is no SOM analysis for material from the sequence.

A core of the buried peat layer (unit 6) was studied by pollen analysis. The summary pollen percentage diagram of the core can be divided into two local pollen zones, zone 1 and zone 2 (Fig. 15).

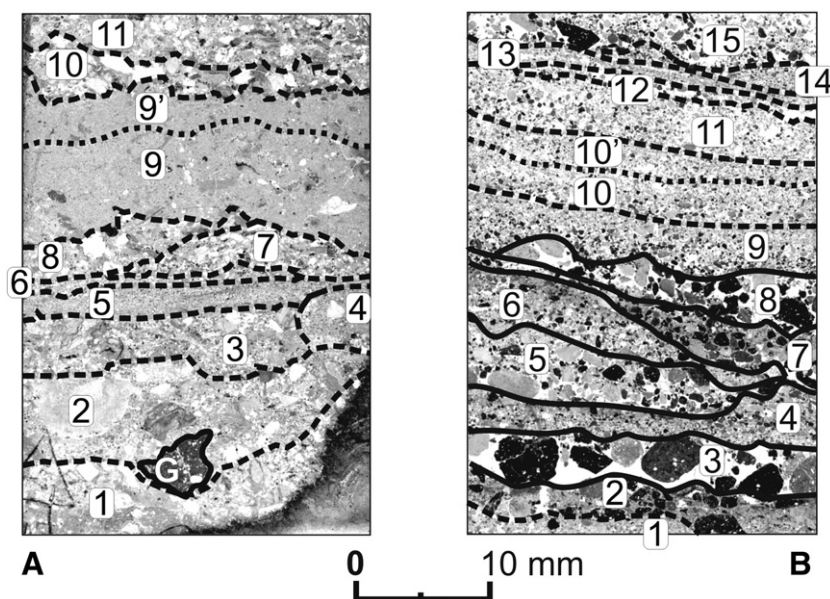


**Fig. 11.** Scanned images obtained from thin sections of Quaternary (A) and contemporary (B) deposits. Images were taken under transmitted light. Numbers indicate the sedimentary units, the transition of which is emphasized by drawing lines. Note glebule (G) at the base of unit 2, in (A), which actually is a fragment of soil aggregate, indicating that the deposit was associated with soil erosion.



**Fig. 12.** Sedimentary pattern of a slope wash deposit, created along the floor of the study clay quarry, after a 60 mm rain event. The deposit was located upslope of the valley head pedostratigraphic sequence, about 50 m away.

Pollen zone 1 (223–188 cm, 4 samples) is characterized by abundant Campos (grassland) pollen taxa (70–85%), primarily Poaceae, followed by Cyperaceae, Asteraceae subf., Asteroideae and *Baccharis*. *Araucaria* Forest pollen sums are moderate (10–20%), represented primarily by Melastomataceae and *Myrsine*, followed by *Weinmannia* and Myrtaceae. Pollen grains of *Araucaria angustifolia* are missing. The representation of Atlantic Forest pollen taxa are low (1–3%) with some single grains such as *Alchornea* and Moraceae/Urticaceae. Tree fern spores of *Cyathea* and *Dicksonia* are recorded in low percentages. Other fern spores are more frequent, primarily represented by the *Blechnum imperiale*-type and monlete psilate spores.

In pollen zone 2 (188–152 cm, 4 samples) pollen of the Campos vegetation are still frequent (50–60%), but markedly less so than in zone 1. Percentages of Poaceae decrease while Cyperaceae percentages increase at the top of the core. Other Campos pollen taxa remain unchanged. The sum of the *Araucaria* Forest group increase, especially by Myrtaceae and *Weinmannia*. Also, other *Araucaria* Forest taxa appear, such as the *Lamanonia speciosa*-type, *Clethra*, the *Symplocus tenuifolia*-type and *S. lanceolata*-type. Percentages of the group of Atlantic rain forest taxa remain at low levels (1–2%). Ferns such as *Blechnum imperiale*-type decrease in this zone, while tree fern *Dicksonia sellowiana* and Monolete psilate percentages increase, followed by *Cyathea* and Trilete psilate types.

This Late-glacial age pollen record suggests a change from an older period with a relatively dry and cold climate (pollen zone 1), before  $^{14}\text{C}$  11.8 ky, to a younger period with a wetter and warmer climate (pollen zone 2), ending at  $^{14}\text{C}$  11.3 ky. This is reflected by a change from Campos with some gallery forest towards larger areas of *Araucaria* forest, mainly in the form of gallery forest along the valley. The general expansion of the gallery forest, the increase of tree ferns such as

*Dicksonia sellowiana* and *Weinmannia* trees also indicates wetter and warmer conditions during the pollen zone 2 period. Since the top of the deposit is missing, probably truncated by erosion before burial, no further conjecture is possible at this time.

Globally, this first order valley sequence bears evidence of shallow braided channel sedimentation around TL 86 ky. This LGC deposit was covered by peat, formed in a shallow swampy environment at the site valley bottom, at least around the Late Pleistocene ( $>^{14}\text{C}$  11.8 ky BP to  $^{14}\text{C}$  11.3 ky BP). Radiocarbon ages, together with pollen record, indicate a relatively rapid change in vegetation composition, in about 500 years, which coincides with the end of the northern hemisphere's Younger Dryas. The peat deposit was partially truncated and covered by undated overbank deposits characteristic of single thread channels, suggesting a switch from an earlier braided system, passing from a swampy environment, to a low-energy fluvial single thread system.

### 3.2. Stratigraphic correlation

Based on measured ages, the different pedostratigraphic sequences were superposed in a graphic sedimentary log (Fig. 16) that presents the maximum thickness of the main layers at each site, as well as their general characteristics. Organized as such, the study deposits may be divided in three different sequences: Lower Sequence, Intermediate Sequence and Upper Sequence.

As suggested by Fig. 16, the study ages coincide with a relatively wide LGC time span, embracing several recognized climatic events in both hemispheres, such as marine isotopic stages (MIS 5, MIS 3, MIS 2 and MIS 1), substages (5c, 5b, 5a), millennial oscillations on climate improvement periods (Bølling/Allerød interstadials; warming trend before Antarctic Cold Reversal) and Late Pleistocene events (Younger Dryas) (Bond et al., 1993; Blunier et al., 1998; Blunier and Brooks, 2001; Cortese and Abelmann, 2002). The study record is truncated, as usual, and one radiocarbon age is technically ambiguous, but the sedimentary source-to sink pathway of the study near-valley head sites is definitely short and coincidences seem consistent. In addition, independent radiocarbon and luminescence ages reported for all three Southern Brazilian States (Paraná; Santa Catarina; Rio Grande do Sul) also suggest the likeliness of a regional signal in Southern Brazil (Fig. 17), probably linking erosive and sedimentary events to global and hemispheric climatic trends, which could be summarized as follows, according to Fig. 16 idealized sedimentary sequence.

#### 3.2.1. The Lower Sequence

a) About TL 90 ky to 86 ky: erosion of weathered mantles and deposition of gravels with subsidiary cross-lamination on slopes and adjacent valleys. Correlative global and hemispheric events: MIS 5b stadial (N.H.) and change from interstadial to stadial condition (S.H.) (Aharon and Chappell, 1986; Cortese and Abelmann, 2002). Possible scenario: erosion and deposition by rain-washing and flash floods in slopes and valleys, during stadial transition. b) About  $^{14}\text{C}$  49 ky BP, or earlier ( $>50$  ky): peat development and proxy evidence (pollen and isotopes) for a relatively wet local environment, with changes in temperature and humidity during the period (from drier and warmer towards wetter and colder). Correlative global and hemispheric events: abrupt climatic oscillations in a longer-term cooling trend; Dansgaard-Oeschger stadials (N.H.) and interstadial oscillations (S.H.) of MIS 3 interstadial (Bond et al., 1993; Peterson et al., 2000; Cortese and Abelmann, 2002). Possible scenario: abrupt changes during a local MIS 3 interstadial that was colder than today, but still humid enough to develop and preserve peat deposits on valley heads. c) About  $^{14}\text{C}$  38 ky BP: development of ochric epipedon on valley heads and proxy isotopic evidence of local vegetation rarefaction. Correlative global and hemispheric events: same as above, during MIS 3 (Bond et al., 1993). Possible scenario: although colder than today, relatively warm and dry climate during one of the MIS 3 southern hemisphere interstadial oscillations. The limit between Lower and Intermediate Sequences

**Table 4**  
Main textural characteristics of units depicted in samples of holocenic and contemporary deposits

Sample	Unit	Main textural characteristics (inner organization–sorting–clast–support–grain size)	Correlation (r) between textural characteristics of lamina (°)
Holocenic (A)	11	Massive, moderately sorted, polymodal matrix-supported coarse sand	Holocenic lamina (A)
"	10	Massive, well sorted, polymodal matrix-supported gravel	
"	9'	Massive very well sorted clay	Texture and clast-support: $r=0.24$
"	9	Normal graded, very well sorted, matrix-supported sandy clays to silty clay	Texture and sorting: $r=0.72$
"	8	Normal graded, well sorted, polymodal clast-supported medium to coarse rounded sand	Texture and organization: $r=0.30$
"	7	Lateral graded, well sorted, polymodal clast-supported elongated medium sand	Clast-Support and sorting: $r=0.34$
"	6	Massive, well sorted, bimodal clast-supported fine sand	Clast-Support and Organization: $r=0.06$
"	5	Finely laminated, well sorted, polymodal matrix-supported sandy silt. Inclined lamination	Sorting and organization: $r=0.27$
"	4	Massive, moderately sorted, polymodal matrix-supported silty sand	
"	3	Massive, well sorted, polymodal matrix-supported very coarse to coarse sand, laterally grading to medium and fine sand	
"	2	Massive, poorly sorted, polymodal clast-supported fine gravel to very coarse sand. Poorly sorted sandy matrix, grading upward. Soil aggregate fragment (G – glebule) at the base of unit	
"	1	Massive, poorly sorted, polymodal matrix-supported fine gravel to very coarse sand	
Contemporary (B)	15	Normal graded, moderately sorted, polymodal clast-supported coarse to medium sand	Contemporary lamina (B)
"	14	Massive, well sorted, bimodal clast-supported fine sand	
"	13	Laminated, well sorted, polymodal matrix-supported sandy silt	Texture and clast-support: $r=0.36$
"	12	Massive, very well sorted, clast-supported medium sand	Texture and sorting: $r=0.14$
"	11	Normal graded, well sorted, polymodal clast-supported medium sand	Texture and organization: $r=0.18$
"	10'	Inverse graded, moderately sorted, polymodal clast-supported medium to fine sand	Clast-support and sorting: $r=0.26$
"	10	Normal graded, well sorted, polymodal clast-supported medium sand	Clast-support and organization: $r=0.35$
"	9	Normal graded, very well sorted, polymodal clast-supported medium to fine sand	Sorting and organization: $r=0.03$
"	8	Massive, very well sorted, bimodal clast-supported very coarse sand	
"	7	Massive, poorly sorted, polymodal matrix-supported coarse silty sand	
"	6	Normal graded, poorly sorted, polymodal clast-supported coarse to medium sand	
"	5	Lateral graded, moderately sorted, bimodal clast-supported very coarse to medium sand	
"	4	Massive, moderately sorted, bimodal clast-supported fine sand	
"	3	Massive, very well sorted, bimodal clast-supported gravel	
"	2	Massive, poorly sorted, polymodal matrix-supported silty sand and gravel	
"	1	Massive, well sorted, polymodal clast-supported medium sands	

<sup>a</sup> The correlation index  $r$  was obtained by the attribution of arbitrary integers for each class of textural characteristics.

(Fig. 16) may be determined by the stratigraphic site-discordance created around OSL 6.6 ky, but a causal relationship with any other obliterated erosive or depositional event is not to be discarded.

3.2.2. The Intermediate Sequence

a) About <sup>14</sup>C19 ky BP: diffusive colluvial deposition; development of thick umbric epipedons and proxy evidence (isotopic) of mixed grasslands and forests (Cerrado) near the study drainage divides. Correlative global event: MIS 2 last glacial maximum (LGM) in both hemispheres (Sowers and Bender, 1995). Possible scenario: morphogenesis and pedogenesis in a local environment colder and dryer than

today, but still humid enough to develop thick umbric epipedons and enable the establishment of trees and bushes around summital areas. b) About <sup>14</sup>C 15.3 ky BP: scattered colluviation and umbric epipedon development, followed by a change of local slope hydrology, passing from diffuse mass movements towards gully erosion and cut-and-fill structures. Correlative global and hemispheric events: climatic improvement between MIS 2 and MIS 1; stadial period before Bølling–Allerød interstadials (N.H.) and warming trend before the Antarctic Cold Reversal Oscillation (S.H.) (Sowers and Bender, 1995; Blunier et al., 1997). Possible scenario: adaptation of hydrogeomorphic systems during period of warming trend (Climatic Improvement),

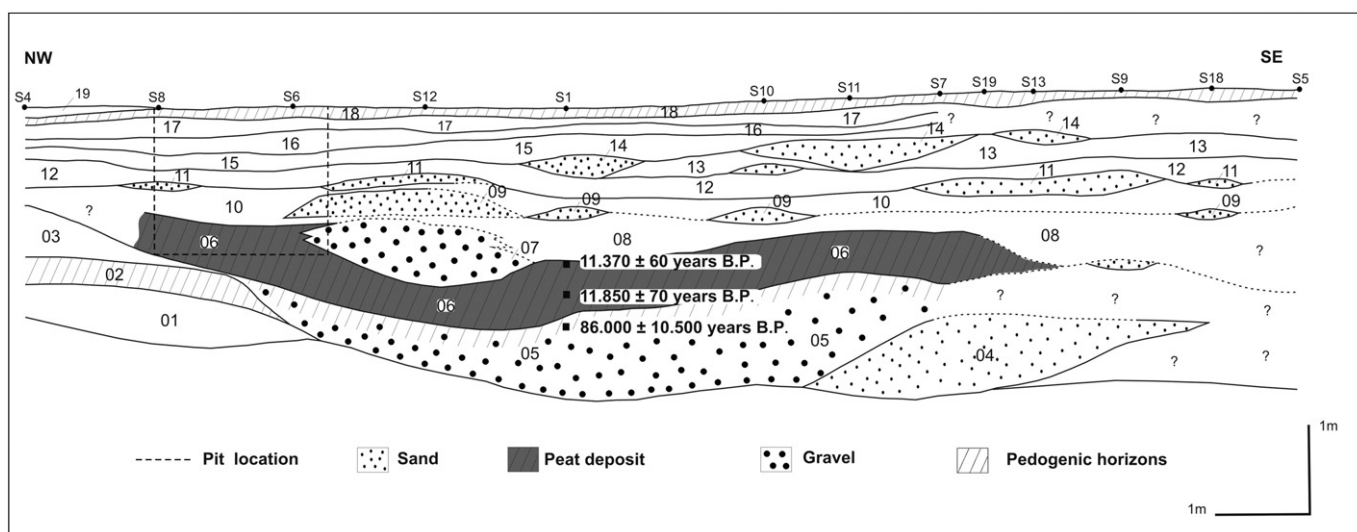


**Fig. 13.** Schematic representation of the valley bottom pedostratigraphic sequence. Numbers correspond to main sedimentary units. The sequence was surveyed by manual drillings. One pit was excavated for sampling and to check detailed structures.

**Table 5**  
Data for radiocarbon ages of valley bottom sequence samples

Laboratory code (#)	Beta 203292
Field code (#)	NE-F6-AM16
Depth of the sample (m)	1.88
Stratigraphic unit	6 (Middle)
Analysis	Radiometric
Age ( <sup>14</sup> C years BP)	11,850 ± 70
δ <sup>13</sup> C (‰)	-18.8

approaching Termination I (Schaefer et al., 2006). c) Between <sup>14</sup>C 11.8 ky BP and <sup>14</sup>C 11.3 ky BP: peat development in a swampy valley environment; proxy pollinic evidence of local climatic change from colder and dry towards warmer and wetter conditions. Correlative global and hemispheric events: end of the Younger Dryas (N.H.), Late Pleistocene oscillations (S.H.) (Broecker, 1995; Sugden et al., 2005). Possible scenario: rapid response of vegetation to climatic amelioration and lower energy depositional environments near the valley heads in a period correlative to the end of N.H. Younger Dryas. There is a gap in the study Intermediate Sequence, between 15.3 ky and 11.3 ky that prevents interpretation about the transition between the Climatic Improvement period and the eventual onset of the Late Pleistocene Younger Dryas. The limit between the Intermediate and Superior Sequences (Fig. 16) may be defined either by the OSL 6.6 ky stratigraphic discontinuity, or by any other erosive event among <sup>14</sup>C 15.3 ky and <sup>14</sup>C 11.3 ky.

3.2.3. The Upper Sequence

a) About OSL 6.6 ky: soil erosion; sedimentologic and micromorphologic evidence of dry conditions and wildfires; relatively thick well stratified rain-wash deposits on aggrading bare footslopes. Correlative global and hemispheric evidence: Hypsithermal (N.H.); warmer climates, either dry or wet (S.H.) (Iriondo, 1999). Possible scenario: local mid Holocene dryness and a seasonal, contrasted climatic regime.

4. Discussion

4.1. Highland near-valley head climate constraints in Southern Brazil

Since no consistent evidence of local influence of tectonism has come to light so far, the study's near-valley head stratigraphic record seems related to the adaptation by local geomorphic systems to environmental constraints that coincide with global and hemispheric climatic changes. This adaptation to climate-driven factors seems to follow a pattern in which important changes in erosion, sedimentation and pollen taxa production tend to cluster around periods of transition between stadials and interstadials, whatever the sign of the climatic change, although warming periods seem to produce more important geomorphogenic responses. During climatic "steady-state" periods, such as interstadials and stadials, ochric and umbric epipedons and peat deposits formed, in addition to less expressive diffusive colluviation (Fernandes and Dietrich, 1996). This general pattern, if correct, is probably due to local responses of geomorphic systems to changes in the principal South American first-order climatic systems:

**Table 6**  
Data for luminescence age of the valley bottom sequence sample

Laboratory code (#)	LVD-1128
Field code (#)	CA-Terraço
Depth of the sample (m)	2.4
Stratigraphic unit	5
Dating method	TL
Annual dose (μCg/yr)	1.150 ± 26
P (Gy)	100
Age (years)	86,000 ± 10,500

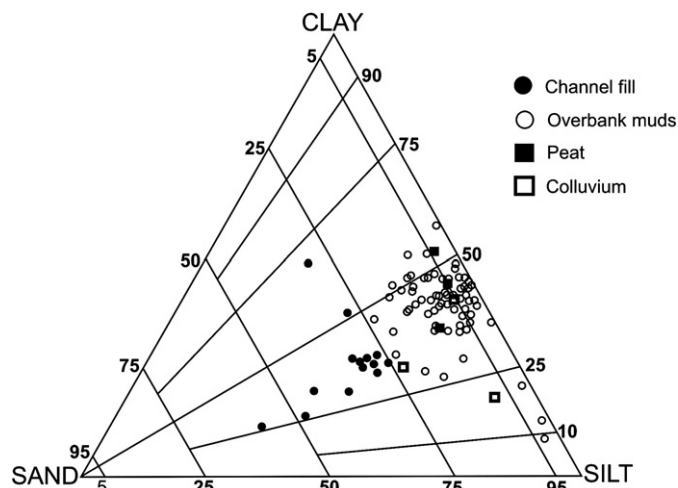


**Fig. 14.** Flemming textural classification of materials from the valley bottom sedimentary sequence. Different genetic deposits tend to cluster in different zones.

the ITCZ, the trade-winds and the three oceanic anticyclones: Azores (AA), South Atlantic (SAA) and South Pacific (SPA).

The record of climatic changes in the South American plains between MIS 4 and Little Ice Age was summarized by Iriondo (1999) who identifies the influence of two main climatic pattern types, derived from present-day dynamics of South-American climatic systems. On the basis of previously published data, the author points to an inversed correlated climatic signal between northern and southern South America during Quaternary climatic oscillations. This inversed signal is explained as a consequence of the preponderant influence either of the southern Pampean climatic type pattern (P), or of the northern Venezuelan climatic type pattern (V). Comparison between events reported by Iriondo (1999) and the study events is illustrated by Table 7.

As far as the information reported in Table 7 coincide, events in the study highlands fit better with the Patagonian (P) pattern, in agreement with Iriondo's climatic types distribution in South America (Iriondo, 1999, p. 110), although coincidence seems stronger during irregular oscillating periods (MIS 3, Climatic Improvement, Late Pleistocene-Y.D.). During "steady-state" stages (MIS 2 and Hypsithermal) a mixed Venezuelan (V) pattern seems to preponderate. Generally, these coincidences are coherent with the previously mentioned apparent pattern of adaptation of the study geomorphic systems to climate-driven factors, where periods of transition would lead to morphogenesis while "steady" periods would induce umbric epipedon and peat formation.

The explanation may be controversial, but probably relates to the balancing effects of cold southern air masses and continental or oceanic tropical air masses around the study area (Grimm et al., 2000). The strong South America latitudinal asymmetry, caused by warm ocean waters in the North and cold ocean currents in the South (Iriondo, 1999), would tend to reinforce effects of regional temperature gradients during irregular oscillating periods, or transitions, enabling expansion of the Patagonian (P) pattern to lower latitudes, either as a result of spreading colder and denser southern air masses, or as a consequence of weakening SAA influence. Tropical continental and oceanic air masses would tend to increase in influence during "steady-state" periods, either cold or warm, pushing the Venezuelan climatic pattern (V) southwards.

Reported results from the Cariaco Basin, off the Venezuelan coast, suggest that increased precipitation and river discharges are closely linked to MIS 3 interstadial abrupt shifts, as recorded in Greenland ice cores (Peterson et al., 2000). This would also suggest that northern South America climatic changes would be synchronous to the

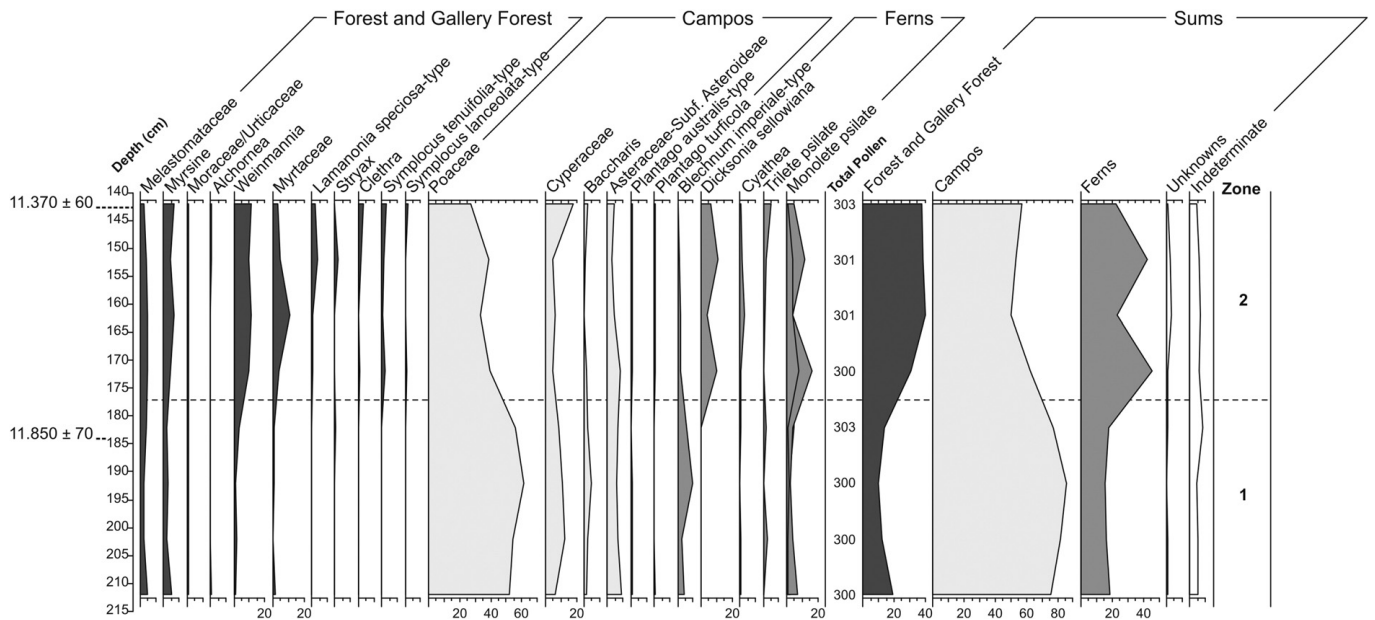


Fig. 15. Pollen diagram and summary pollen percentage diagram of unit 6 buried peat layer in the valley bottom pedostratigraphic sequence.

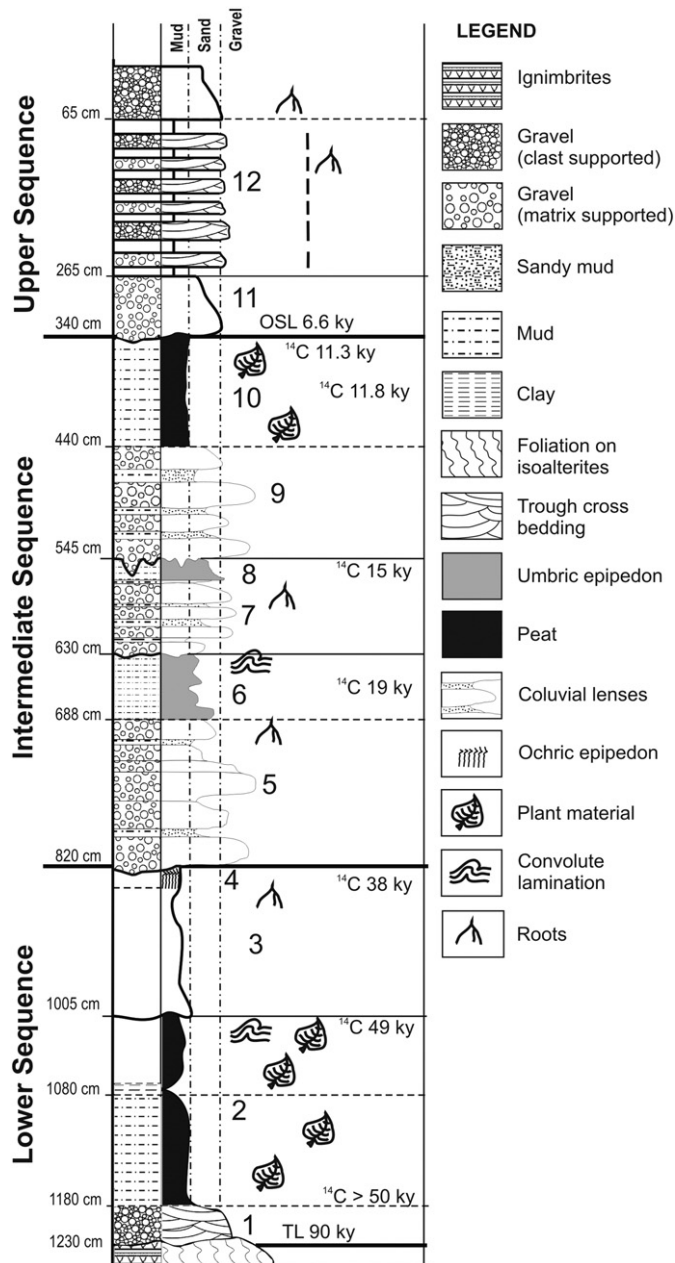


Fig. 16. Idealized sedimentary log of all study pedostratigraphic sequence's deposits. The numbers indicate the main sedimentary units, ordered by their age.

northern hemisphere's major climatic changes, emphasizing the existence of far-reaching teleconnection effects that link Milankovich's "sensitive latitudes" to equatorial climate, or vice-versa. Evidence of a mixed Venezuelan "V" pattern at the study LGM and MIS 1 record, during "steady state" periods, may be viewed as another example of the teleconnection hypothesis. However, the reasons why the study record suggests an extending influence of the "V" pattern climate to areas where the "P" pattern would be expected (Iriondo, 1999) are still not clear enough for further conjecture.

Iriondo's bi-polar model also predicts local transient climatic conditions. Concerning the study area, these local conditions may be important, since the sites locate near the watersheds, about 1000 m a. s.l., in valley heads of very small catchments, perched between the steep Atlantic *Serra do Mar* ranges and the gentle westerly dipping Southern Brazilian Plateau highlands. Under these circumstances, Atlantic Polar Cold Front migration and local orographic effects may be equally important controlling factors, influencing the response of

hydrogeomorphic systems. This is probably the case for the evidence found in this study of dryness during the mid Holocene, as well as for the relatively wet conditions during MIS 3 and LGM.

Independent interpretation for the "Serra Campos Gerais" pollen record had suggested a Holocene palaeoclimate with a long dry season (Behling, 1997a). This may also have been the case for the study sites, where no annual dry season occurs under modern climatic conditions. This climatic condition with a marked seasonal dry period in early and mid Holocene could be explained by a stronger influence from dry, tropical continental air masses in Southern Brazil (Behling, 1993), which would have blocked polar cold fronts farther south preventing precipitation over the study area. Evidence of longer dry seasons in the early Holocene were also found in different records from S and SE Brazil (Servant et al., 1989; Behling, 1997b; Pessenda et al., 2004; Melo and Cuchierato, 2004; Moro et al., 2004), suggesting a regional trend which points to possible future local effects of current global climatic warming. In addition, according to models run by Wasson and Claussen (2002) this relative early-mid Holocene dryness would be expected to occur in Australia and Africa, at similar latitudes, and even at lower ones, as suggested by the short arid pulses depicted by high-amplitude lake regressions in the main Ethiopian rift during the period (Benvenuti et al., 2002).

The chronology of the study near-valley head stratigraphic record is coincident with global and hemispheric events depicted in Greenland and Antarctic ice caps (Bard et al., 1997; Blunier et al., 1998; Blunier and Brooks, 2001; Clark et al., 2002; Weaver et al., 2003). Conjecture about major regional climatic factors may explain why transitions between stadial and interstadial periods seem to be associated with erosion and rain-wash deposition in the study slopes and valleys, probably under the influence of contrasted seasonal climatic regimes. Organic-rich soils and peat deposits, which need conditions of water saturation for several months to fully develop (Shotyk, 1992), are present in every sequence of the study. Their ages coincide with LGC periods when global temperature was lower than today, which is also supported by the study proxy data, suggesting the existence of shallow soil-water saturated zones in topographic hollows under the influence of local wet environments, low temperatures and low evaporation rates. This local wet soil-environment condition would tend to maintain overland flow as an efficient and recurrent mechanism through time, also explaining the dynamics of alternate periods of pedogenesis and morphogenesis at the study valley heads, implying anaerobic soil development during climatic stable periods and soil erosion and local deposition under transient climate conditions.

### 5. Conclusions

The study sites witness an important LGC stratigraphic record, which give evidence of the adaptation of near-valley head areas to climate-driven processes in the humid tropics. Due to their relative scarcity in Quaternary colluvial-alluvial stratigraphy studies, a number of results deserve mention: a) evidence of erosion and sedimentation at early LGC stages; b) evidence of sedimentation and pedogenesis during the LGM; c) evidence of hydrogeomorphic changes during the Climatic Improvement, between MIS 2 and MIS 1; d) sedimentary evidence of pronounced dryness, at least under contrasted seasonal regimes, during the mid Holocene; e) evidence of rain-washing as an important geomorphic agent since the end of MIS 3, at least, until the mid Holocene; f) evidence of mixed grasslands and forests around LGM topographic summits; g) pollinic, isotopic and sedimentologic evidence of climate changes more complex than the "warming and wet vs. cooling and dry" classic binomial model for the humid tropics; h) evidence of secular adaptation of vegetation and geomorphic systems to climatic changes at the Late Pleistocene.

To our knowledge, no similar near-valley head stratigraphic record had been reported before in Brazil, and few in other countries embrace

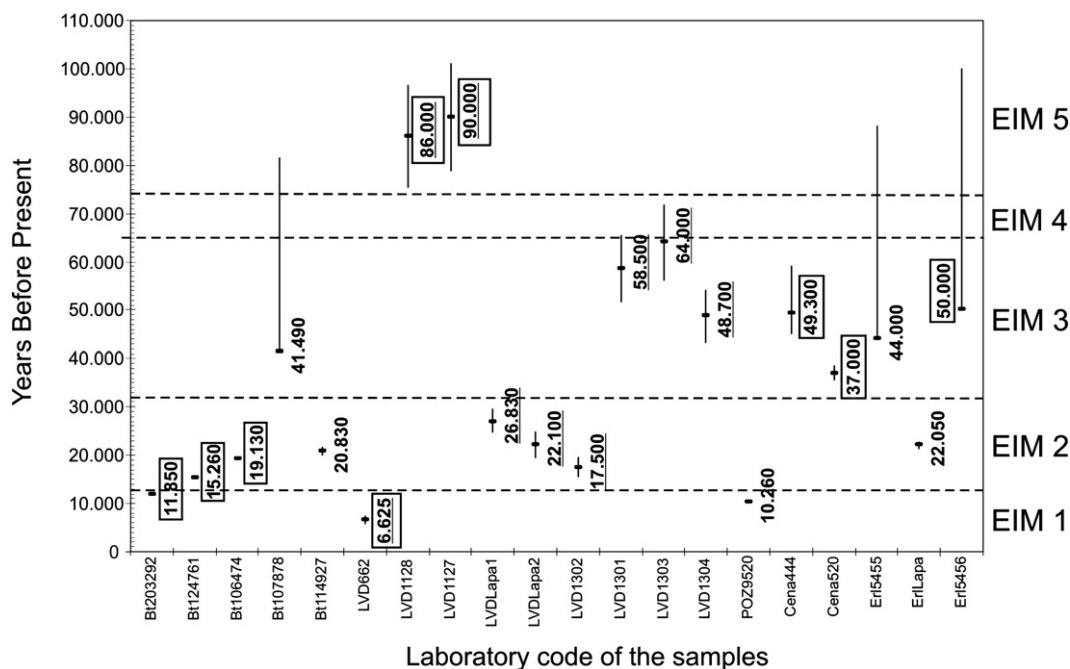


**Fig. 17.** Independent radiocarbon and luminescence ages reported for the Southern Brazilian States of Paraná, Santa Catarina and Rio Grande do Sul. Luminescence ages are underlined. The ages inside the rectangles refer to study results. Note the distribution of dating with respect to main Late Pleistocene marine isotopic stages (MIS). The figure was compiled after Oliveira et al. (2001), Camargo (2005), Camargo Filho (2005) and Fett (2005).

such a wide site-to-site time span. The interpretation stresses the influence of very local controlling factors that seem to respond to regional and global climatic-driven processes. Under similar local environmental conditions, the observed sedimentary pattern may reflect regional trends, affecting southern Brazilian highlands. This pattern suggests that near-valley head slopes and channels had evolved under the influence of local shallow soil-water saturated zones. Stadials would imply drier climate periods, but lower temperatures and lower evaporation rates still would support local saturated zones, improving the development of umbric epipedons, the formation of peat deposits and pulses of overland flow and mass movements on the slopes. During dryer periods, mostly warming but also cooling, rain-wash erosion would be more influential.

This recurrent concentration of hydrologic-driven processes through time is perhaps one of the most important influences of valley head areas on the adaptation of drainage net systems to environmental changes (Dietrich and Dunne, 1993). As a result, near-valley head areas deserve further attention in Quaternary studies since, besides their alleged sensitiveness and resilience, these areas also express unambiguous short source-to-sink sedimentary path-

ways, generally improving the quality of the stratigraphic record. The Southern Brazilian highlands, under relatively mild climate today, probably constitute a special terrain for preservation and study of near-valley head Quaternary deposits. The verification of a similar record in other countries may represent a clear contribution of geomorphology to the improvement of Quaternary studies.

**Acknowledgement**

This research was supported by CNPq (Brazilian National Research Council).

**References**

Aharon, P., Chappell, J., 1986. Oxygen isotope sea-level changes and the temperature history of a coral reef environment in New Guinea over the last 10<sup>5</sup> years. *Palaeogeography, Palaeoclimatology, Palaeoecology* 56, 337–352.  
 Bard, E., Rostek, F., Sonzogni, C., 1997. Interhemispheric synchrony of the last deglaciation inferred from alkenone palaeothermometry. *Nature* 385, 707–710.  
 Behling, H., 1993. Untersuchungen zur spätpleistozänen und holozänen Vegetations- und Klimageschichte der tropischen Küstenwälder und der Araukarienwälder in

**Table 7**  
 Comparison between South America LGC events reported by Iriondo (1999) and events deduced from the study sedimentary sequences

Late Quaternary stage	Patagonian pattern (P)	Venezuelan pattern (V)	Study highlands pattern
MIS 5	No mention	No mention	Stadial, or stadial transition. Flash floods on slopes and valleys
MIS 4	Cold. Extremely stable dryness	Oscillating cold and warm climates	No mention
MIS 3	Warming climate with 3 major alternated events (humid/dry/humid)	Cold, followed by irregular climatic improvement and glacial events	Colder than today and humid. 3 stratigraphic events (peat; mud deposits; ochric epipedon). Warming and drying to the end of IS.
MIS 2	Similar to MIS 4	Cold and wet before 23 ky. Glacial events between 23 ky and 19.5 ky	Cold. Although dryer, relatively wet at 19.5 ky
Climatic improvement	Increasing humidity by 15–16 ky	Lower temperatures and dry climate before 13 ky	Cold, but increasing humidity after 15 ky
Late Pleistocene (Younger Dryas)	Increasing dryness and torrential events	Warm and humid (12.25 ky–11.96 ky). Cold and humid (11.7 ky–9.51 ky)	Late Glacial conditions (dryer) switch to humid climate in few centuries (11.8 ky–11.3 ky), with low-energy fluvial single thread system
Hypsithermal	Warm and humid climate. Floods and swamps in accretionary dynamics	Warm and humid (9.35 ky–6.2 ky). Cold and dry (6.2 ky–5.8 ky)	Increasing dryness. Seasonal regimes and wildfires (6.6 ky)

- Santa Catarina (Südbrasilien). *Dissertationes Botanicae* 206, J. Cramer, Berlin, Stuttgart.
- Behling, H., 1997a. Late Quaternary vegetation, climate and fire history in the *Araucaria* forest and campos region from Serra Campos Gerais (Paraná), S Brazil. *Review of Palaeobotany and Palynology* 97, 109–121.
- Behling, H., 1997b. Late Quaternary vegetation, climate and fire history from the tropical mountain region of Morro de Itapecva, SE Brazil. *Palaeogeography, Palaeoclimatology, Palaeoecology* 129 (3–4), 407–422.
- Benvenuti, M., Carnicelli, S., Belluomini, G., Dainelli, N., Di Grazia, S., Ferrari, G.A., Iasio, M., Sagri, M., Ventra, D., Atnafu, Balemwald, Kebede, Seifu, 2002. The Ziway-Shala lake basin (main Ethiopian rift, Ethiopia): a revision of basin evolution with special reference to the Late Quaternary. *Journal of African Earth Sciences* 35, 247–269.
- Bertran, P., Texier, J.P., 1999. Facies and microfacies of slope deposits. *Catena* 35, 99–121.
- Bertran, P., Jomelli, V., 2000. Post-glacial colluvium in western Norway: depositional processes, facies and palaeoclimatic record. *Sedimentology* 47, 1053–1068.
- Bigarella, J.J., Mousinho, M.R., 1965. Considerações a respeito dos terraços fluviais, rampas de colúvio e várzeas. *Boletim Paranaense de Geografia* 16/17, 153–197.
- Biondi, J.C., Bartoszek, M.K., Vanzela, G.A., 2001. Controles geológicos e geomorfológicos dos depósitos de caulim da bacia de Campo Alegre (SC). *Revista Brasileira de Geociências* 31, 13–20.
- Blunier, T., Brooks, E.J., 2001. Timing of millennial-scale climate change in Antarctica and Greenland during the Last Glacial period. *Science* 291, 109–112.
- Blunier, T., Schwander, I., Stocker, T.F., Dallenbach, A., Indermuhle, A., Tschumi, J., Chappellaz, I., Raynaud, D., Barnola, J.M., 1997. Timing of the Antarctic atmospheric CO<sub>2</sub> increase with respect to the Younger Dryas event. *Geophysical Research Letters* 24, 2683–2686.
- Blunier, T., Chappellaz, I., Schwander, I., Dallenbach, A., Stauffer, B., Stocker, T.F., Raynaud, D., Jouzel, J., Clausen, H.B., Hammer, C.U., Johnsen, S.J., 1998. Asynchrony of Antarctica and Greenland climate during the last glacial. *Nature* 394, 739–743.
- Bond, G., Broecker, W., Johnsen, S., McManus, J., Labeyrie, L., Jouzel, J., Bonani, G., 1993. Correlations between climate records from North Atlantic sediments and Greenland ice. *Nature* 365, 143–147.
- Broecker, W.S., 1995. Cooling the tropics. *Nature* 376, 212–213.
- Bullock, P., Fedoroff, N., Jongerius, A., Stoops, G., Tursina, T., 1985. *Handbook of soil thin section description*. Waine Research, Albrington.
- Camargo, G., 2005. O significado paleoambiental de depósitos de encosta e de preenchimento de canal no município de Lapa, no sul do Segundo Planalto Paranaense. Ph.D. Thesis, Geografia - Universidade Federal de Santa Catarina, Florianópolis, Santa Catarina, Brazil.
- Camargo Filho, M., 2005. O significado paleoambiental de seqüência pedosedimentar em baixa-encosta: o caso dos paleossolos Monjolo, Lapa, PR. Ph.D. Thesis, Geografia - Universidade Federal de Santa Catarina, Florianópolis, Santa Catarina, Brazil.
- Clark, P.U., Mitrovica, J.X., Milne, G.A., Tamisiea, M.E., 2002. Sea-Level Fingerprinting as a direct test for the source of Global Meltwater Pulse IA. *Science* 295, 2438–2441.
- Coltrinar, L., 1993. Global Quaternary changes in South America. *Global and Planetary Change* 7, 11–23.
- Cortese, G., Abelman, A., 2002. Radiolarian-based paleotemperatures during the last 160 kyr at ODP site 1089 (Southern Ocean, Atlantic Sector). *Palaeogeography, Palaeoclimatology, Palaeoecology* 182, 259–286.
- De Keyser, T.L., 1999. Digital scanning of thin sections and peels. *Journal of Sedimentary Research* 69, 962–964.
- Delvigne, J., 1998. *Atlas of Micromorphology of Mineral Alteration and Weathering*. The Canadian Mineralogist, Special publication 3, Mineralogical Association of Canada and ORSTOM Éditions.
- Dietrich, W.E., Dunne, T., 1993. The channel head. In: Beven, K., Kirkby, M.J. (Eds.), *Channel network hydrology*. John Wiley and Sons, New York, pp. 175–219.
- Fard, A.M., 2001. Recognition of abrupt climate changes in clastic sedimentary environments: an introduction. *Global and Planetary Change* 28, 9–12.
- Fernandes, N.F., Dietrich, W.E., 1996. Modeling hillslope evolution under cyclic climatic oscillations: the time required to steady-state. *Anais da Academia Brasileira de Ciências* 68, 157–162.
- Ferreira, G.M.S.S., Oliveira, M.A.T., 2006. Aplicação da micromorfologia de solos ao estudo de sedimentos alúvio-cólvios em cabeceiras de vale. *Pesquisas em Geociências* 33 (2), 3–18.
- Fett, N. Jr., 2005. Aspectos morfológicos, estratigráficos e sedimentológicos de depósitos quaternários no curso médio do Rio Pardo (município de Candelária, RS). M.Sc. Thesis, Geografia - Universidade Federal de Santa Catarina, Florianópolis, Santa Catarina, Brazil.
- Finkl Jr., C.W., 1984. Chronology of weathered materials and soil age determination in pedostratigraphic sequences. *Chemical Geology* 44 (1–3), 311–335.
- Fleming, B.W., 2000. A revised textural classification of gravel-free muddy sediments on the basis of ternary diagrams. *Continental Shelf Research* 20, 1125–1137.
- Folk, R.L., 1974. *The petrology of sedimentary rocks*. Hemphill Publishing Co., Austin.
- Grimm, E.C., 1987. Coniss: a Fortran 77 program for stratigraphically constrained cluster analysis by the method of the incremental sum of squares. *Computer and Geosciences* 13, 13–35.
- Grimm, A.M., Barros, V.R., Doyle, M.E., 2000. Climate variability in Southern South America associated with El Niño and La Niña events. *Journal of Climate* 13, 35–58.
- Iriondo, M., 1999. Climatic changes in the South American plains: records of a continent-scale oscillation. *Quaternary International* 57/58, 93–112.
- Lima, G.L., 2005. Caracterização pedostratigráfica de depósitos de encosta e de vale, localidade de Cerro do Touro, Campo Alegre, Estado de Santa Catarina. M.Sc. Thesis, Geografia - Universidade Federal de Santa Catarina, Florianópolis, Santa Catarina, Brazil.
- Meis, M.R.M., Machado, M.B., 1978. A morfologia de rampas e terraços do Médio Vale do Rio Doce. *Finisterra* 13, 201–218.
- Meis, M.R.M., Monteiro, A.M.F., 1979. Upper Quaternary "Rampas", Doce River Valley, SE Brazilian Plateau. *Zeitschrift für Geomorphologie* 232, 132–151.
- Meis, M.R.M., Moura, J.R.S., 1984. Upper quaternary sedimentation and hillslope evolution: Southeastern Brazilian plateau. *American Journal of Science* 284, 241–254.
- Melo, M.S., Cuchierato, G., 2004. Quaternary colluvial-eluvial covers of the Eastern Paraná Basin, Southeastern Brazil. *Quaternary International* 114, 45–53.
- Melo, M.S., Coimbra, A.M., Cuchierato, G., 2001. Genesis of Quaternary colluvial-eluvial covers in Southeastern Brazil. *Quaternaire* 12 (3), 179–188.
- Miall, A.D., 1985. Architectural-element analysis: a new method of facies analysis applied to fluvial deposits. *Earth Science Reviews* 22, 261–308.
- Modenesi-Gautieri, M.C., 2000. Hillslope deposits and the Quaternary evolution of the *Altos Campos* - Serra da Mantiqueira, from Campo do Jordão to the Itatiaia Massif. *Revista Brasileira de Geociências* 30, 504–510.
- Moro, R.S., Bicudo, C.E.M., Melo, M.S., Schmitt, J., 2004. Paleoclimate of the late Pleistocene and Holocene at Lagoa Dourada, Paraná State, southern Brazil. *Quaternary International* 114, 87–99.
- Moura, J.R.S., Mello, C.L., 1991. Classificação aloestratigráfica do Quaternário Superior da região de Bananal (SP/RJ). *Revista Brasileira de Geociências* 21 (3), 236–254.
- Moura, J.R.S., Peixoto, M.N.O., Silva, T.M., 1991. Geometria do relevo e estratigrafia do Quaternário como base à tipologia de cabeceiras de drenagem em anfiteatro - Médio Vale do Rio Paraíba do Sul. *Revista Brasileira de Geociências* 21 (3), 255–265.
- Nemec, W., Kazanci, N., 1999. Quaternary colluvium in west-central Anatolia: sedimentary facies and palaeoclimatic significance. *Sedimentology* 46, 139–170.
- Oliveira, M.A.T., Pereira, K.N., 1998. Identificação de Solos Colúvios em Áreas de Cabeceira de Drenagem: Cerro do Touro, Campo Alegre (SC). *Revista Geosul* 14 (27), 476–481.
- Oliveira, M.A.T., Lima, G.L., 2004. Classificação de sedimentos quaternários em cabeceiras de vale através da aplicação do diagrama de Flemming: município de Campo Alegre, Norte de Santa Catarina. *Revista Geociências* 23 (1/2), 67–78.
- Oliveira, M.A.T., Camargo, G., Paisani, J.C., Camargo Filho, M., 2001. Caracterização paleohidrológica de estruturas sedimentares quaternárias através de análises macroscópicas e microscópicas: do registro sedimentar local aos indícios de mudanças globais. *Pesquisas em Geociências* 28, 183–195.
- Oliveira, M.A.T., Pessenda, L.C.R., Behling, H., Lima, G.L., Ferreira, G.M.S.S., 2006. Registro de mudanças ambientais pleistocênicas e holocênicas em depósitos de cabeceira de vale: Campo Alegre, Planalto Norte catarinense (SC). *Revista Brasileira de Geociências* 36 (2), 474–487.
- Pessenda, L.C.R., Gouveia, S.E.M., Aravena, R., Boulet, R., Valencia, E.P.E., 2004. Holocene fire and vegetation changes in southeastern Brazil as deduced from fossil charcoal and soil carbon isotopes. *Quaternary International* 114 (9), 35–43.
- Peterson, L.C., Haug, G.H., Hughen, K.A., Röhl, U., 2000. Rapid changes in the hydrologic cycle of the tropical Atlantic during the last glacial. *Science* 290, 1947–1951.
- Schaefer, J.M., Denton, G.H., Barrel, D.J.A., Ivy-Ochs, S., Kubik, P.W., Andersen, B.G., Philips, F.M., Lowell, T.V., Schlüchter, C., 2006. Near-synchronous interhemispheric termination of the last glacial maximum in mid-latitudes. *Science* 312 (5779), 1510–1513.
- Scholle, P.A., 1979. *A color illustrated guide to constituents, textures, cements and porosities of sandstones and associated rocks*. American Association of Petroleum Geologists, Memoir 28, Tulsa.
- Servant, M., Soubiès, F., Suguio, K., Turcq, B., Fournier, M., 1989. Alluvial fans in Southeastern Brazil as an evidence for early Holocene dry climate period. *International Symposium on Global Changes in South America During the Quaternary, Special Publication 1*. ABEQUA-INQUA, São Paulo, pp. 75–77.
- Shotyk, W., 1992. Organic soils. In: Martini, I.P., Chesworth, W. (Eds.), *Weathering, Soils and Paleosoils*. Developments in Earth Surface Processes, vol. 2. Elsevier, Amsterdam, pp. 203–224.
- Sowers, T.A., Bender, M., 1995. Climate records covering the last glaciation. *Science* 269, 210–214.
- Stevaux, J.C., Santos, M.L., 1998. Palaeohydrological changes in the Upper Paraná River, Brazil, during the late Quaternary: a facies approach. In: Benito, G., Baker, V.R., Gregory, K.J. (Eds.), *Palaeohydrology and Environmental Change*. John Wiley and Sons, Chichester, pp. 273–285.
- Sugden, D.E., Bentley, M.J., Fogwill, C.J., Hulton, N.R.J., McCulloch, R.D., Purves, R.S., 2005. Late-glacial glacier events in southernmost South America: a blend of "northern" and "southern" hemispheric signals? *Geografiska Annaler* 87(A), 273–288.
- Thomas, M.F., 2004. Landscape sensitivity to rapid environmental change - a Quaternary perspective with examples from tropical areas. *Catena* 55, 107–124.
- Thomas, M.F., Thorp, M.B., 1996. The response of geomorphic systems to climate and hydrological change during the Late Glacial and early Holocene in the humid and sub-humid tropics. In: Branson, J., Thomas, M.F., Nott, J., Price, D.M. (Eds.), *Global Continental Changes: the Context of Palaeohydrology*, Geological Society Special Publication 115. London, pp. 139–154.
- Thomas, M.F., Nott, J., Price, D.M., 2001. Late Quaternary sedimentation in the humid tropics: a review with new data from NE Queensland, Australia. *Geomorphology* 39, 53–68.
- Turcq, B., Pressinotti, M.N., Martin, L., 1997. Paleohydrology and paleoclimate of the past 33,000 years at the Tamanduá river, Central Brazil. *Quaternary Research* 47, 284–294.
- Wasson, R.J., Claussen, M., 2002. Earth system models: a test using the mid-Holocene in the Southern Hemisphere. *Quaternary Science Reviews* 21, 819–824.
- Weaver, A.J., Saenko, O.A., Clark, P.U., Mitrovica, J.X., 2003. Meltwater pulse 1A from Antarctica as a trigger of the Bölling-Allerød warm interval. *Science* 299, 1709–1713.